NMR study in the superconducting silicon clathrate compound $Na_xBa_ySi_{46}$

Fumihiko Shimizu,* Yutaka Maniwa, and Kiyoshi Kume
Department of Physics, Faculty of Science, Tokyo Metropolitan University, Minami-osawa, Hachioji, Tokyo 192-03, Japan

Hitoshi Kawaji, Shoji Yamanaka, and Mitsuo Ishikawa
Department of Applied Chemistry, Faculty of Engineering, Hiroshima University, Higashi-Hiroshima 739, Japan
(Received 30 January 1996; revised manuscript received 15 July 1996)

^{29}Si, ^{23}Na, ^{137}Ba, and ^{135}Ba NMR experiments were carried out in the superconducting silicon clathrate compound $Na_xBa_ySi_{46}$ to study the electronic states above the superconducting transition temperature. We observed three distinct ^{29}Si signals with different Knight shift (2036, 862, and 720 ppm at 90 K with a small temperature dependence of ~10%), which were ascribed to inequivalent Si sites in the Si_{46} structure. The results indicate that the conduction-electron spin and/or charge density is strongly site-dependent. At all the atomic sites, the Korringa relation in NMR relaxation was observed, indicative of metallic electronic structure with moderate electronic correlation. The Na and Ba atoms are partially ionized in $Na_xBa_ySi_{46}$, which shows the noticeable difference from the system of alkali-metal-doped fullerides. The comparison with band calculations is discussed. [S0163-1829(96)06042-0]

I. INTRODUCTION

The recent discovery of superconductivity in alkali-metal-doped fullerides[1] inspired a hope of superconductivity in silicon clathrate compounds M_xSi_{46} and M_xSi_{136} (M=alkali metal) whose crystalline structure consists of Si polyhedral cages. The physical properties of these fullerene-related compounds were investigated many years ago.[2,3] Although the expected high Debye frequency for the tetrahedrally coordinated Si network should be favorable for the superconductivity of the BCS mechanism, no evidence of the transition was found down to 2 K.[4] More recently, new types of silicon clathrate compounds codoped with Ba, $M_xBa_ySi_{46}$, were synthesized,[5] and were found to undergo superconducting transition at about 4 K.[6] To our knowledge, this is the first observation of superconductivity in the system which consists of the sp^3 covalent network of silicon.

As shown in Fig. 1, the Si_{46} structure is given by filling in space with silicon polyhedra; dodecahedra (Si_{20}) and tetrakaidecahedra (Si_{24}) are linked to each other, sharing their pentagonal or hexagonal faces. It was revealed by x-ray Rietveld analysis[5] that the Ba atoms occupy the center of the tetrakaidecahedra, while the Na atoms occupy mainly the center of the dodecahedra. If all the tetrakaidecahedra and the dodecahedra were exactly occupied by Ba atoms and Na atoms, respectively, one would have the composition of $Na_2Ba_6Si_{46}$.

The fact that the introduction of a Ba atom resulted in the occurrence of the superconductivity suggests an important role of the alkaline-earth metal.[7] This point was supported by a theoretical study. Based on the density-functional theory with the local-density approximation (LDA), an electronic structure calculation in $Na_2Ba_6Si_{46}$ (Ref. 8) showed that the strong hybridization of the Ba states with the Si_{46} states yields high Fermi-level density of states $N(E_F)$, which was supposed to be of essential importance for the superconductivity. Experimentally, on the other hand, detailed investigation on the electronic states in $M_xBa_ySi_{46}$ has not yet been made.

In the present work, we carried out ^{29}Si, ^{23}Na, ^{137}Ba, and ^{135}Ba NMR experiments in $Na_xBa_ySi_{46}$ to study the electronic states above the superconducting transition temperature (T_c). At all the atomic sites, considerable Knight shift K_S was observed, and NMR spin-lattice relaxation rate T_1^{-1} was found to obey the Korringa relation, which is indicative of metallic electronic structure. These results verify that the Si_{46} states at the Fermi level have a large amount of s component, consistent with the Si-sp^3 hybrid orbital, and indicate that the Na atoms are partially ionized as well as the Ba atoms. These features are noticeably different from the case of alkali-metal-doped fullerides, in which the s character of

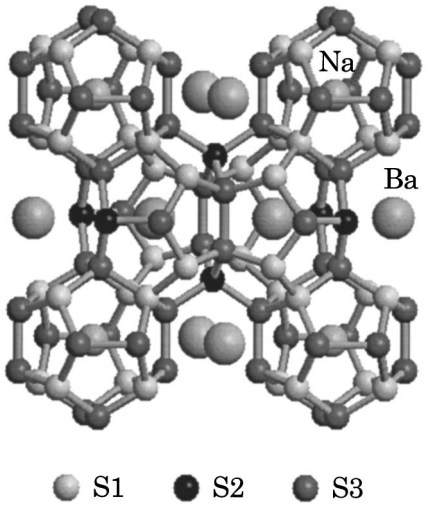

FIG. 1. The structure of $Na_2Ba_6Si_{46}$. The largest spheres are Ba atoms occupying the center of tetrakaidecahedron, and the smaller spheres located at the center of the dodecahedron are Na atoms. There are three kinds of inequivalent Si sites: $S1$, $S2$, and $S3$ (see text).

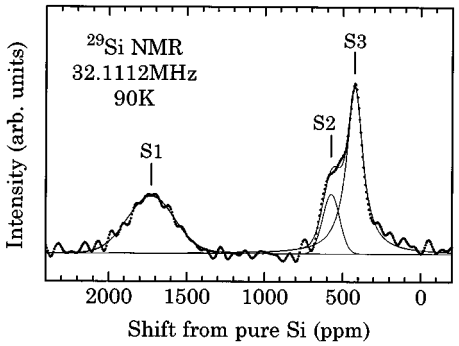

FIG. 2. ^{29}Si NMR spectrum at 90 K. The NMR shift is measured from the resonance in the semiconducting pure Si. The vertical line shows the peak position of each signal of the inequivalent Si sites. The solid lines display the result of fitting by Gaussian curve (for the $S1$ and $S2$ site) and Lorentzian one (for $S3$ site), whose areas are in the ratio of 16:6:24.

the conduction-electron wave functions at Fermi level is weak,[9,10] and the alkali metals are almost completely ionized.[11] The small deviation of $T_1TK_s^2$ from the Fermi-contact value for noninteracting electrons shows that the normal state of $Na_xBa_ySi_{46}$ is an ordinary simple metal with moderate electronic correlation.

II. EXPERIMENT

The sample was synthesized from two kinds of Zintl phase compounds of NaSi and $BaSi_2$. Details of the sample preparation were described in the previous papers.[5,6] The powder sample used contains $BaSi_2$ impurity phase. The composition of the clathrate phase actually determined by the atomic absorption[5] was $Na_{2.9}Ba_{4.5}Si_{46}$, where the excess Na atoms should occupy the tetrakaidecahedra.

The NMR spectra were taken by a home-built Fourier transform spectrometer at the magnetic field of 3.79 T. Instead of an ordinary NMR glass tube which contains Si and Na, Si- and Na-free sample tubes were used. In addition to the sample containing $BaSi_2$ impurity phase, we measured NMR spectra in the $BaSi_2$ starting material as well, and it was confirmed that the influence of the impurity on both ^{29}Si and ^{137}Ba NMR could be neglected.

III. RESULTS AND DISCUSSION

We shall first discuss the results for ^{29}Si NMR experiments. Figure 2 shows the spectrum taken at 90 K. The NMR shift was measured with respect to the ^{29}Si resonance in semiconducting pure Si at room temperature (-68 ppm from TMS). In the Si_{46} structure, there are three kinds of inequivalent Si sites which are the possible origins of distinct NMR signals, as shown in Fig. 1. We shall call these groups $S1$, $S2$, and $S3$, whose numbers of sites are in the ratio of 16:6:24. $S1$ site belongs to the dodecahedral Si_{20} cage and gives the direct Si-Si bond between Si_{20} cages; $S2$ site is not included in the Si_{20} cage; $S3$ site belongs to the Si_{20} cage and gives the Si-Si bond between the $S2$ site and the Si_{20} cage. The assignment of the spectrum was made on the basis of the integrated intensity (Fig. 2). The positions of the resonance lines vary with temperature by $\sim$10% as shown in Fig. 3. In

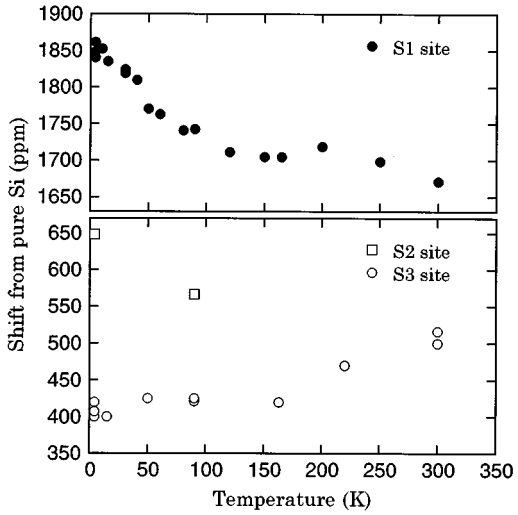

FIG. 3. Temperature variation of the peak positions of the resonance lines of Si-$S1$ site (closed circle), Si-$S2$ site (square), and Si-$S3$ site (open circle).

the following analysis, the shift K is divided into spin part K_s and orbital part (chemical shift) K_c, i.e., $K=K_s+K_c$. The observation of considerable Knight shifts at the Si sites, as shown below, verifies that the Si_{46} states at the Fermi level consist of the Si-sp^3 orbital fairly having s character, in contrast to fullerene compounds in which the conduction band mainly consists of carbon π orbital.[9,10]

Figure 4 shows the temperature dependence of ^{29}Si NMR spin-lattice relaxation rate T_1^{-1}, along with that of ^{137}Ba and ^{23}Na, which is discussed later. The relaxation rate was mainly measured by the conventional saturation recovery method. At all the measuring points, magnetization recovery data could be fitted by single exponential curves. It is found that the Korringa-like relation $T_1T=$const approximately holds at each Si site. For Si-sp^3 orbital, the contributions

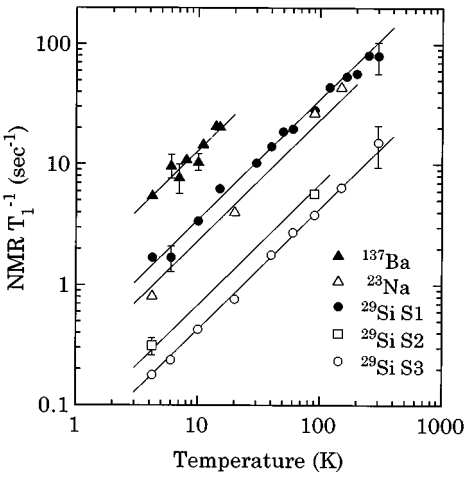

FIG. 4. Temperature dependence of ^{29}Si, ^{23}Na, and ^{137}Ba NMR spin-lattice relaxation rate T_1^{-1}; Si-$S1$ site (closed circle), Si-$S2$ site (square), Si-$S3$ site (open circle), Ba site (closed triangle), and Na site (open triangle). The solid lines which display the relation $T_1T=$const are guide for the eyes.

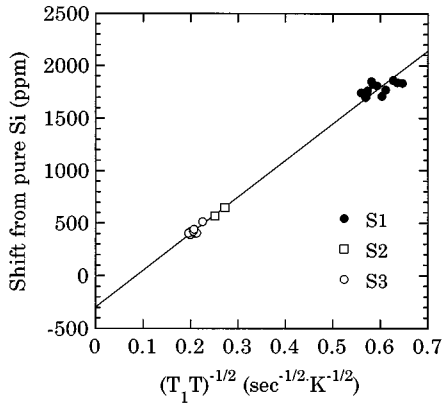

FIG. 5. ^{29}Si NMR shift as a function of $(T_1T)^{-1/2}$. The symbols are the same as Fig. 3. The different points for the same kind of Si site correspond to different temperatures.

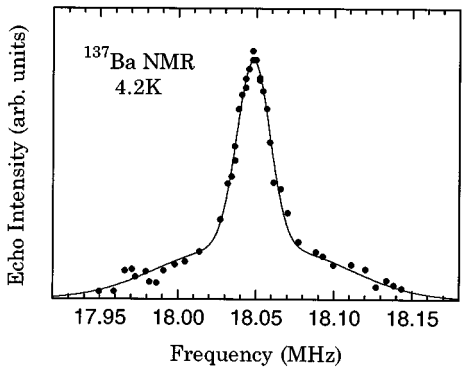

FIG. 6. ^{137}Ba NMR spectrum at 4.2 K measured by the point-to-point method. The line shape is considered to be the powder pattern of first-order quadrupolar broadening. The solid line shows the result of fitting, in which the central line is fitted by Gaussian, and the satellite lines are also broadened by Gaussian with different width.

from the Fermi-contact, dipole, and orbital interactions to the relaxation can be roughly estimated.[12] The relaxation rate due to Fermi-contact interaction $(T_1^{-1})_s$ is given by

$$(T_1^{-1})_S = \tfrac{64}{9}\pi^3\gamma_e^2\gamma_N^2\hbar^3\langle|u_{\mathbf{k}}(0)|^2\rangle^2[N_s(E_F)]^2k_BT, \quad (1)$$

where γ_e and γ_N are the electronic and nuclear gyromagnetic ratio, respectively, $|u_{\mathbf{k}}(0)|^2$ is the electronic density at the atomic position for state $\mathbf{k}$, $\langle\ \rangle$ means taking the average over the Fermi surface, and $N_s(E_F)$ is the Fermi-level density of states per one spin direction. Neglecting the matrix elements between the neighboring sp^3 orbitals, we have the relaxation rate due to dipole interaction $(T_1^{-1})_{\rm dip}$ as follows:

$$(T_1^{-1})_{\rm dip} = \tfrac{9}{50}\pi\gamma_e^2\gamma_N^2\hbar^3\langle r^{-3}\rangle^2[N_s(E_F)]^2k_BT, \quad (2)$$

where $\langle r^{-3}\rangle$ is the expectation value of r^{-3} for the sp^3 orbital averaged over the Fermi surface. By use of the literature value of $|\psi(0)|^2=1.38$ (in atomic units) which was experimentally deduced for the conduction electron of doped Si (Ref. 13) and the Hartree-Fock value of $\langle r^{-3}\rangle_{3p}=2.0541$ for neutral Si atom,[14] the $(T_1^{-1})_s$ is estimated to be about 180 times larger than the $(T_1^{-1})_{\rm dip}$. Since the relaxation rate due to orbital interaction $(T_1^{-1})_{\rm orb}$ is also estimated to be negligible compared with $(T_1^{-1})_s$, we can conclude that the ^{29}Si NMR relaxation is dominated by the Fermi-contact interaction.

For the analysis of the shift, the shifts of the different kinds of Si sites at various temperatures are plotted as a function of $(T_1T)^{-1/2}$ in Fig. 5. The data points can be fitted well by a straight line. On the assumption of the same amount of K_c for the different kinds of Si sites, the straight line in the plot implies that the T_1^{-1} obeys the Korringa relation, $T_1TK_s^2=S\alpha$, where S is Korringa's Fermi-contact value for noninteracting electrons, being 6.66×10^{-6} sec K for ^{29}Si nucleus, and α is the measure of deviation from the simple Korringa relation. The negative intercept of -296 ppm is K_c, and the slope of the line gives α, being 1.8. Thus, we have the Knight shift K_s at 90 K, for example, to be 2036, 862, and 720 ppm for $S1$, $S2$, and $S3$, respectively. The value of α is quite close to those of ordinary simple metals such as alkali metals, indicating that the electronic correlation is not very strong.

Now, we shall turn to the metals encapsulated into the silicon polyhedra. Unlike ^{29}Si nucleus with the spin of $\frac{1}{2}$, both of the nuclei of ^{137}Ba and ^{23}Na have the spin of $I=\frac{3}{2}$. Figure 6 shows the ^{137}Ba NMR spectrum measured by the point-to-point method at 4.2 K. The line shape is interpreted as the powder pattern of a first-order quadrupolar splitting. The observed peak is mainly due to $\frac{1}{2}$ to $-\frac{1}{2}$ transition (central line). By the powder pattern with appropriate Gaussian broadening, we could reproduce the line shape as displayed by the solid line in the figure. From the fitting, we obtained 176 kHz for $\nu_Q=e^2qQ/h$, where eq is electric field gradient at Ba nucleus and eQ is electric quadrupole moment of ^{137}Ba. In order to verify this interpretation, we measured ^{135}Ba NMR as well, and the spectrum with similar line shape was obtained. The ratio of the gyromagnetic ratio of ^{137}Ba nucleus to that of ^{135}Ba, $\gamma_{137}/\gamma_{135}$, is 1.12, while the ratio of their quadrupole moments $(eQ)_{137}/(eQ)_{135}$ is 1.7. The frequency ratio of their peak positions is in good agreement with the ratio of $\gamma_{137}/\gamma_{135}$, indicating that the origin of the shift is magnetic. Further, if we assume the first-order quadrupole splitting, the line shape for ^{135}Ba is found to be reproduced by using the same value for the electric field gradient eq. These results confirm the validity of the above interpretation.

The shift of the ^{137}Ba central line measured with respect to the resonance in $BaCl_2$ aqueous solution is 5930 ppm at 4.2 K. This value is larger than that of Ba bulk metal being 4030 ppm, indicating that the dominant contribution is the Knight shift. As shown in Fig. 7(a), the shift of the central line was found to decrease with increasing temperature between 4.2 and 30 K. For ^{23}Na NMR, the resonance line was found around 900 ppm with a reference of $1M$-NaCl aqueous solution. The observed shift is comparable to that of Na metal, and is evidently beyond a range of the chemical shift of ^{23}Na. This also indicates the dominant contribution of the Knight shift for the observed shift. This result shows that considerable charge density of the conduction electron with s character remains at the Na site, whereas the LDA calculation[8] predicted that the Na site in $Na_2Ba_6Si_{46}$ is the lowest density area of the conduction electrons.

^{137}Ba NMR spin-lattice relaxation rate T_1^{-1} was measured by saturating the central line. Evidently, the recovery curve of the central line was not single exponential. For the nucleus

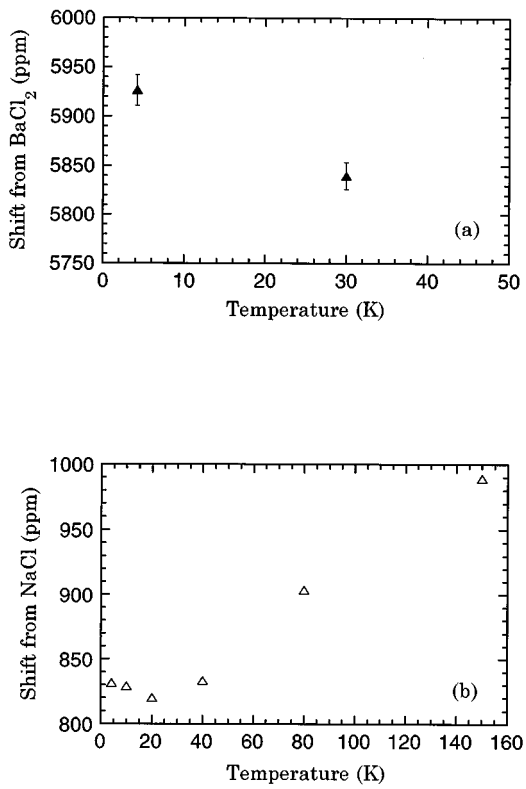

FIG. 7. Temperature variation of the NMR shift of ^{137}Ba (a) and ^{23}Na (b). The ^{137}Ba and ^{23}Na NMR shifts are measured from the resonance lines in $BaCl_2$ and NaCl aqueous solutions, respectively.

of $I=\frac{3}{2}$, if the spin-lattice relaxation is governed by a magnetic interaction, the recovery of nuclear magnetization $M(t)$ with time t after the saturation of the central line is described by the following expression:[15]

$$M(t)=M_0\left\{1-\tfrac{2}{5}\exp\left(-\frac{t}{T_1}\right)-\tfrac{3}{5}\exp\left(-\frac{6t}{T_1}\right)\right\}, \quad (3)$$

where M_0 is the magnetization in thermal equilibrium. If there is a contribution from quadrupolar interaction to the relaxation, the relaxation process should be described by a modified expression, while the obtained data could be fitted by Eq. (3) within the experimental errors, as shown in Fig. 8.

In order to reveal the origin of the relaxation mechanism, we measured ^{135}Ba NMR relaxation rate as well. The recovery data could be again fitted by Eq. (3) as shown in Fig. 8. We obtained 1.5 ± 0.2 for the ratio of the relaxation rates of the two isotopes, $(T_1^{-1})_{137}/(T_1^{-1})_{135}$. This value is closer to that expected for the case of magnetic origin for T_1, $(T_1^{-1})_{137}/(T_1^{-1})_{135}=(\gamma_{137}/\gamma_{135})^2=1.25$, rather than $(T_1^{-1})_{137}/(T_1^{-1})_{135}=[(eQ)_{137}/(eQ)_{135}]^2=2.9$ for the case of electric-quadrupolar origin. Therefore, we concluded that the quadrupolar interaction does not give major contribution to the T_1^{-1}. Because of the poor experimental accuracy, however, we can't accurately determine the amount of the quadrupolar part, so that we tentatively adopted the T_1^{-1}'s determined by Eq. (3). The temperature dependence of ^{137}Ba NMR T_1^{-1} was found to obey the Korringa-like relation, though the data points were limited to a range between 4.2 and 15 K (Fig. 4).

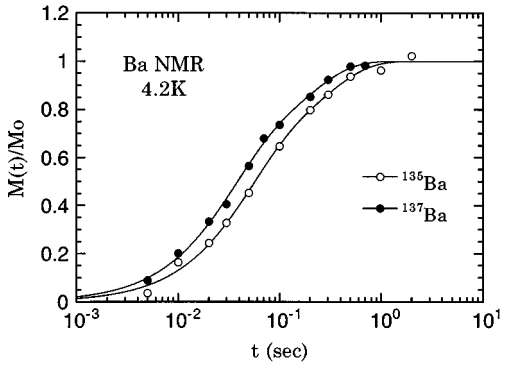

FIG. 8. Magnetization recovery curves for the central lines of ^{135}Ba NMR (open circle) and ^{137}Ba NMR (closed circle) measured at 4.2 K. The solid lines display the results of fitting by Eq. (3) in the text. The magnetization of the ^{137}Ba NMR recovers about 1.5 times faster than that of ^{135}Ba NMR.

For ^{23}Na NMR, the spin-lattice relaxation rate also obeys the Korringa-like relation, approximately. The best fitting of the magnetization recovery data was given by single exponential curves, which indicates that all the resonance lines of ^{23}Na were observed, and that the electric field around the Na site has nearly cubic symmetry. The deviation factor α in the Korringa relation was estimated to be 1.3 for ^{137}Ba and 0.9 for ^{23}Na, provided that the observed shifts from the reference samples are entirely equal to the Knight shifts.

From the Knight shift, the contribution from each atomic state to the Fermi-level density of states can be estimated. On the assumption of noninteracting conduction electrons, the isotropic Knight shift K_s is given by

$$K_S=\frac{8\pi}{3}\langle|u_{\mathbf{k}}(0)|^2\rangle_{E_F}\mu_B^2N(E_F), \quad (4)$$

where μ_B is the Bohr magneton.[16] If one inserts an electronic density normalized within the atomic volume into Eq. (4), one will have a local density of states at the atomic site $n(E_F)$. Using the above-mentioned value of $|\psi(0)|^2=1.38$, we have $n(E_F)=0.50$, 0.22, and 0.18 states/eV site for $S1$, $S2$, and $S3$, respectively. These estimated values should be taken to include both the Si $3s$ and the Si $3p$ components. In this estimation, the hybridizing ratio of the two components was assumed to be the same for all the Si sites. For the Ba site, taking into account only the $6s$ state which is the highest occupied state in the free atom, we have $n(E_F)=0.47$ states/eV site by use of the Hartree-Fock value of $|\psi(0)|^2=4.0878$ for the $6s$ state of Ba^+.[14] For the Na site, $n(E_F)$ was similarly estimated to be 0.57 states/eV site. Summing up these $n(E_F)$'s with respect to the unit cell of $Na_2Ba_6Si_{46}$, we have $N(E_F)=18$ states/eV. This value is considerably lower than the $N(E_F)$ of 47.9 states/eV obtained by the LDA calculation.[8] We believe that this discrepancy could never be explained by the uncertainty in the used $|\psi(0)|^2$'s. For instance, if we use the $|\psi(0)|^2$ of the conduction band of Si deduced from an Overhauser experiment,[17] which is about two times larger than that used above, a smaller $N(E_F)$ by a factor of about 2 than the above estimates is obtained. Saito *et al.*[8] pointed out that, in $Na_2Ba_6Si_{46}$, the Ba $5d$ states rather than the $6s$ states would strongly hybridize

with the Si_{46} states, yielding high Fermi-level density of states. The discrepancy in the density of states may imply that the Ba $5d$ states significantly contribute to the $N(E_F)$.

The above speculation seems to be consistent with the temperature variation of NMR shift as shown in Figs. 3 and 7. The shifts of Si-$S3$ and Na sites increase with temperature. This can be explained by an increase in $N(E_F)$ due to the thermal expansion of the lattice, usually observed in metals. However, for Si-$S1$, Si-$S2$, and Ba sites, oppositely, the shift decreases with increasing temperature. One possible explanation for this variation is due to the temperature-dependent Pauli susceptibility arising from steep energy dependence of the density of states. The LDA calculation is really predicting that the density of states of $Na_2Ba_6Si_{46}$ has steep energy dependence around the Fermi level as the consequence of the strong hybridization of the Ba $5d$ orbital. If this is the case, the Ba $5d$ orbital would hybridize with those at Si-$S1$ and Si-$S2$ sites stronger than Si-$S3$ and Na sites.

In the present work, it was found that $Na_xBa_ySi_{46}$ has metallic electronic structure with moderate electronic correlation. Therefore, the most probable candidate for the mechanism of the superconductivity is naturally considered to be the BCS mechanism. In addition, it has been confirmed that the conduction electrons exist at all of the atomic sites with quite site-dependent amplitude. In the case of alkali-metal-doped fullerides, the complete charge transfer from the alkali metal to the fullerene molecule takes place,[11] and the π-electron system on the carbon spheres is solely responsible for the superconductivity.[9,10] In $Na_xBa_ySi_{46}$, contrastingly, since the Na and Ba orbitals are included into the conduction electron band, they may play a part in the superconductivity in a different manner. Substitution of the Na atom by other alkali-metal atoms may result in the different superconducting properties. $K_xBa_ySi_{46}$ and $Rb_xBa_ySi_{46}$ have been already synthesized,[7] and slightly different T_c's have been reported. In addition, it was reported that, in $Na_xBa_ySi_{46}$, the reduction of the Na-doping level resulted in the higher T_c.[18]

It should be noted that the shift of the $S1$ site is remarkably larger than those of the other Si sites. The ^{29}Si NMR in nonsuperconducting Na_xSi_{136}, now under investigation, is observed around the frequencies for the $S2$ and $S3$ site in $Na_xBa_ySi_{46}$ and not observed around that for the $S1$ site. Therefore, the remarkably large shift of the $S1$ site may be caused by the hybridization with the Ba orbitals and the existence of the Si site with such a large shift in $Na_xBa_ySi_{46}$ might have some relevance to the superconductivity.

ACKNOWLEDGMENTS

This work was supported in part by a Grant-in-Aid from the Ministry of Education, Science and Culture. This work was also supported in part by the Fund for Special Research Project at Tokyo Metropolitan University.

*Present address: Department of Mathematics and Physics, National Defense Academy, 1-10-20 Hashirimizu, Yokosuka 239, Japan.

[1] A. F. Heberd, M. J. Rosseinsky, R. C. Haddon, D. W. Murphy, S. H. Glarum, T. T. M. Palstra, A. P. Ramirez, and A. R. Kortan, Nature (London) **350**, 600 (1991).

[2] J. S. Kasper, P. Hagenmuller, M. Pouchard, and C. Cros, Science **150**, 1713 (1965).

[3] C. Cros, M. Pouchard, and P. Hagenmuller, J. Solid State Chem. **2**, 570 (1970).

[4] S. B. Roy, K. E. Sim, and A. D. Caplin, Philos. Mag. B **65**, 1445 (1992).

[5] S. Yamanaka, H. Horie, H. Nakano, and M. Ishikawa, Fullerene Sci. Tech. **3**, 21 (1995).

[6] H. Kawaji, H. Horie, S. Yamanaka, and M. Ishikawa, Phys. Rev. Lett. **74**, 1427 (1995).

[7] H. Kawaji, H. Horie, S. Yamanaka, and M. Ishikawa (unpublished).

[8] S. Saito and A. Oshiyama, Phys. Rev. B **51**, 2628 (1995).

[9] Y. Maniwa, T. Saito, A. Ohi, K. Mizoguchi, K. Kume, K. Kikuchi, I. Ikemoto, S. Suzuki, Y. Achiba, M. Kosaka, K. Tanigaki, and T. W. Ebbesen, J. Phys. Soc. Jpn. **63**, 1139 (1994).

[10] V. P. Antropov, I. I. Mazin, O. K. Andersen, A. I. Liechtenstein, and O. Jepsen, Phys. Rev. B **47**, 12 373 (1993).

[11] Y. Maniwa, K. Mizoguchi, K. Kume, K. Tanigaki, T. W. Ebbesen, S. Saito, J. Mizuki, J. S. Tsai, and Y. Kubo, Solid State Commun. **82**, 783 (1992).

[12] Y. Obata, J. Phys. Soc. Jpn. **18**, 1020 (1963).

[13] R. G. Shulman and B. J. Wyluda, Phys. Rev. **103**, B1127 (1956).

[14] S. Fraga, J. Karwowski, and K. M. S. Saxena, *Handbook of Atomic Data* (Elsevier, Amsterdam, 1976), p. 291.

[15] E. R. Andrew and D. P. Tunstall, Proc. Phys. Soc. **78**, 1 (1961).

[16] A. Abragam, *Principles of Nuclear Magnetism* (Oxford, New York, 1961).

[17] V. Dyakonov and G. Denninger, Phys. Rev. B **46**, 5008 (1992).

[18] H. Kawaji, K. Iwai, S. Yamanaka, and M. Ishikawa, Solid State Commun. (to be published).